Syntheses and Characterization of Copper(II) Complexes of the New Ligands *N*-[(2-Pyridyl)methyl]-2,2′-dipyridylamine and *N*-[Bis(2-pyridyl)methyl]-2-pyridylamine

Simon P. Foxon,[a] **Olaf Walter,**[b] **and Siegfried Schindler***[a]

Keywords: Copper / Oxygen / Coordination chemistry / Ligand effects / Tripodal ligands

The two new ligands *N*-[(2-pyridyl)methyl]-2,2′-dipyridylamine (**L1**) and *N*-[bis(2-pyridyl)methyl]-2-pyridylamine (**L2**) have been synthesized and the copper(II) complexes $[Cu(\mathbf{L1})_2(CH_3OH)_2](ClO_4)_2$, $[Cu(\mathbf{L1})_2(H_2O)_2](ClO_4)_2$, $[Cu_3(\mathbf{L1})_2(DMF)_2Cl_6]$, $[Cu(\mathbf{L1})Cl_2]_n$, $[Cu(\mathbf{L2})(Cl)(ClO_4)]$, and $[Cu(\mathbf{L2})Cl_2]$ have been structurally characterised. The reactions of dioxygen with the copper(I) complexes with ligands **L1** and **L2** were investigated, but no copper–dioxygen intermediates could be detected spectrophotometrically.

Introduction

A large number of biologically important metalloproteins utilise copper ions in their active sites for the redox-processing of molecular dioxygen.[1−6] Examples include hemocyanin (O_2 carrier in the blood of arthropods and molluscs), tyrosinase (*o*-phenol monooxygenase), and other oxidases, which couple oxidation of the substrate with copper-mediated reduction of dioxygen to hydrogen peroxide or water.[7−11]

The function of the metalloprotein is closely related to the structure of its active site, i.e. the geometrical arrangement of amino acid residues around the copper ions. There has been considerable interest in the design of ligands and the characterisation of copper complexes that may constitute models of the active site structure in such metalloproteins.[1,4−6,12−16] In particular, copper complexes of tris(2-pyridylmethyl)amine (tmpa) and closely related ligands have been widely employed in order to explore and understand the thermodynamic and kinetic aspects of the reaction of copper(I) compounds with dioxygen.[1,17−22]

We recently carried out a detailed study on a family of three ligands closely related to tmpa, in which each "arm" of the tripodal parent ligand tmpa was systematically lengthened by the insertion of a methylene spacer group.[23] This systematic approach allowed an evaluation of the effect of the chelate ring size on the following properties: copper(I)-oxygen reactivity, the coordination geometry around the copper ion, the Cu^{II}/Cu^{I} redox couple, and spectroscopic features (UV/Vis, EPR).

The properties of these complexes were found to be strongly affected by changing the chelate ring size and, therefore, we also became interested in performing a similar investigation in which the tripodal ligand, tmpa, had each "arm" systematically shortened (Scheme 1). The tripodal amine, tris(2-pyridyl)amine (tpa; unfortunately tmpa has also been abbreviated as tpa in the literature) has been known for a long time,[24] but the two ligands *N*-[(2-pyridyl)methyl]-2,2′-dipyridylamine (**L1**) and *N*-[bis(2-pyridyl)methyl]-2-pyridylamine (**L2**), intermediate between tmpa and tpa, are as yet unknown in the literature.

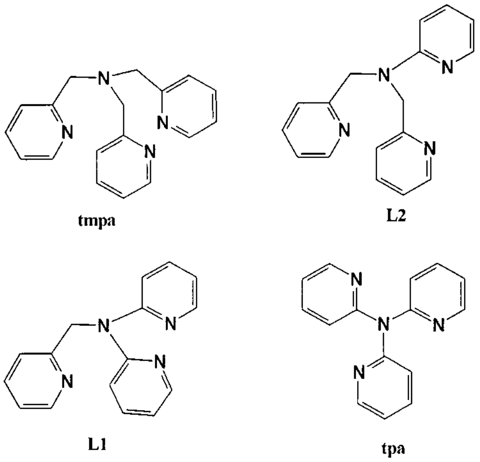

Scheme 1. The ligands tpa, **L1**, **L2**, and tmpa

Herein, we report the synthesis of these two new ligands and the characterisation of their copper(II) complexes, as

---

[a] Institute of Inorganic Chemistry, University of Erlangen-Nürnberg,
Egerlandstraße 1, 91058 Erlangen, Germany
Fax: (internat.) + 49-(0)9131−85 27 387
E-mail: schindls@anorganik.uni-erlangen.de
[b] ITC-CPV, Forschungszentrum Karlsruhe GmbH, ITC-CPV,
Postfach 3640, 76021 Karlsruhe, Germany

1434−1948/02/0101−0111 $ 17.50+.50/0

well as some preliminary studies of the reactivity of the copper(I) complexes with dioxygen.

Results and Discussion

The ligands *N*-[(2-pyridyl)methyl]-2,2′-dipyridylamine (**L1**) and *N*-[bis(2-pyridyl)methyl]-2-pyridylamine (**L2**) were synthesized by nucleophilic substitution reactions of the precursor amines with 2-picolyl chloride (Scheme 2). The resulting ligands were isolated in multigram quantities in modest yields. The two ligands are crystalline solids and were obtained in a highly pure state by recrystallisation from an appropriate solvent (see Exp. Sect.).

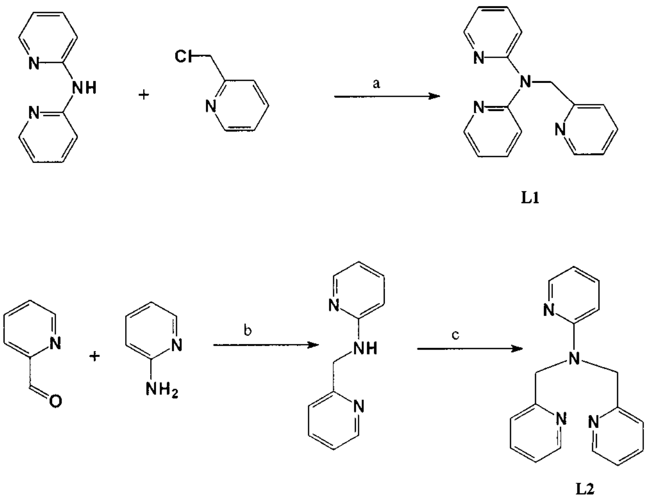

Scheme 2. Synthesis of the ligands **L1** and **L2**; reagents and conditions: **a**: KOH/DMSO, room temp., 2 h. **b**: i. benzene, reflux, 18 h, ii. $NaBH_4$, 18 h. **c**: i. NaH, DMF, room temp., 1 h, ii. picolyl chloride, DMF, room temp., 18 h

The copper(II) complexes used in this study were prepared by adding a copper(II) salt to the appropriate ligand. Crystals suitable for single-crystal X-ray diffraction studies were obtained either by slow evaporation of the solvent(s) from solutions in methanol, water, acetonitrile, or mixtures thereof, or by slow diffusion of diethyl ether into solutions of the complexes in DMF or acetonitrile.

L1 is a versatile ligand. It incorporates rigidity in the form of the dipyridyl moiety, while "flexibility" is provided by the pendant pyridyl "arm". The dipyridyl moiety of **L1** acts as a rigid bidentate donor to the copper(II) centres and it is observed that in the structures presented herein, the third pyridyl nitrogen atom does not coordinate to the same copper(II) centre. We demonstrate in this work that by changing the solvent and counteranions a variety of unique and different structures incorporating the common motif of ligand **L1** can readily be prepared.

Ligand **L2** is closely related to bis(2-pyridylmethyl)amine (dipica), but has been derivatised by the incorporation of an extra pyridine moiety. This introduces the possibility of additional coordination and hence the formation of new coordination compounds.

It should be noted that the proposed formulae obtained on the basis of elemental analyses of the copper(II) complexes differ from the structures obtained by single-crystal X-ray diffraction studies. This is due to the removal of solvent molecules from the crystal lattices in preparing samples for elemental analysis.

X-ray Structures

A summary of the crystallographic data and refinement parameters for the structures reported in this study can be found in Table 1. Selected bond lengths and angles for the copper(II) complexes are reported in Table 2.

Ligand L1

Crystals of **L1** were obtained by slow evaporation of the solvent from a solution of the ligand in acetonitrile at room temperature. An ORTEP representation of the crystal structure of ligand **L1** is shown in Figure 1. The crystal structure of **L1** shows no extraordinary features and is comparable to the reported structures of tpa and its derivatives.[25,26]

$[Cu(L1)_2(CH_3OH)_2](ClO_4)_2$ (1a)

Blue block-shaped crystals of **1a** were grown by slow diffusion of diethyl ether into a solution of the complex in DMF/methanol. The structure of the cation of **1a** is shown in Figure 2, while the coordination parameters around the copper(II) centre are listed in Table 2.

The structure of **1a** (Figure 2) reveals that two molecules of **L1** coordinate to the central copper(II) ion. Each **L1** molecule coordinates to the copper(II) centre through the two pyridine nitrogen atoms, N(2) and N(3), of the dipyridyl moiety. Due to the copper ion occupying a crystallographic inversion centre, the coordinated pyridyl nitrogen atoms and the copper(II) ion are rigorously coplanar. The equatorial ligands form a rectangular rather than a square basal plane around the copper(II) ion, as is evident from the N−N distances [$N(2)-N(3)^i$ = 2.9627(13) Å, N(2)−N(3) = 2.7365(13) Å]. Two methanol molecules are coordinated to the copper(II) ion in the axial positions. The resulting geometry around the copper(II) coordination sphere in **1a** can be described as elongated tetragonal [Cu(1)−N(2) = 2.0181(13) Å, Cu(1)−N(3) = 2.0150(13) Å, Cu(1)−O(1) = 2.4187(13) Å], which is characteristic of d^9 hexacoordinate copper(II) complexes. Furthermore, the methanol molecules are not perpendicular to the equatorial plane, which is evident from the angles [N(3)−Cu(1)−O(1) = 94.41(5)°, $N(3)^i-Cu(1)-O(1)$ = 85.59(5)°], with each methanol molecule being *slightly* tilted towards the uncoordinated pyridyl moiety. This is perhaps unsurprising, considering the interesting and unexpected observation of a strong *intramolecular* hydrogen bonding interaction between the "pendant" pyridyl nitrogen N(4) and O(1) of the methanol molecule in the structure of **1a** [O(1)···N(4) = 2.7472(13) Å].

Although methanol is not a particularly good ligand, especially when bound at the axial coordination positions of the Jahn−Teller sensitive copper(II) ion, metal-bound methanol molecules have been observed in transition metal

Table 1. Crystallographic data from the X-ray diffraction studies of **L1**, **1a−1d**, **2a**, and **2b**

	L1	1a	1b	1c	1d	2a	2b
Empirical formula	$C_{16}H_{14}N_4$	$C_{34}H_{36}Cl_2CuN_8O_{10}$	$C_{38}H_{46}Cl_2CuN_{10}O_{12}$	$C_{44}H_{56}Cl_6Cu_3N_{12}O_4$	$C_{16}H_{14}Cl_2CuN_4$	$C_{17}H_{16}Cl_2CuN_4O_4$	$C_{17}H_{18}Cl_2CuN_4O$
M_r	262.31	851.14	969.28	1220.32	396.75	474.78	428.79
Temperature [K]	200(2)	200(2)	200(2)	200(2)	200(2)	200(2)	200(2)
Radiation used (λ [Å])	Mo-K_α (0.71073)	Mo-K_α (0.71073)	Mo-K_α (0.71073)	Mo-K_α (0.71073)	Mo-K_α (0.71073)	Mo-K_α (0.71073)	Mo-K_α (0.71073)
Crystal description	colourless block	blue block	blue block	blue block	green plates	green block	green plates
Crystal size [mm]	0.6 × 0.6 × 0.3	0.6 × 0.6 × 0.4	0.8 × 0.8 × 0.5	0.3 × 0.2 × 0.2	0.4 × 0.1 × 0.1	0.2 × 0.2 × 0.2	0.3 × 0.3 × 0.2
Crystal system	monoclinic	triclinic	monoclinic	triclinic	monoclinic	monoclinic	monoclinic
Space group	$P2_1/n$ (No. 14)	$P\bar{1}$ (No. 2)	$C2/c$ (No. 15)	$P\bar{1}$ (No. 2)	$P2(1)$ (No. 4)	$P2_1/n$ (No. 14)	$P2_1/n$ (No. 14)
a [Å]	8.976(3)	9.1818(5)	23.377(2)	8.9545(19)	7.6273(12)	8.2210(5)	8.6690(8)
b [Å]	15.083(6)	9.9260(6)	13.6502(13)	12.024(2)	13.947(2)	14.6760(9)	11.8603(11)
c [Å]	10.354(2)	11.2268(6)	14.4648(14)	13.303(3)	7.9549(13)	15.4302(9)	17.1999(16)
α [°]	90	71.3840(10)	90	82.53(2)	90	90	90
β [°]	111.61(2)	78.2960(10)	108.3600(10)	81.60(2)	111.556(2)	102.1950(10)	91.7060(13)
γ [°]	90	69.0490(10)	90	69.17(2)	90	90	90
V [Å^3]	1303.3(7)	900.99(9)	4380.7(7)	1319.6(5)	787.1(2)	1819.67(19)	1767.7(3)
Z	4	1	4	1	2	4	4
F(000)	552	439	2012	625	402	964	876
$\rho_{calcd.}$ [g·cm^{-3}]	1.337	1.569	1.470	1.536	1.674	1.733	1.611
μ [mm^{-1}]	0.083	0.825	0.693	1.555	1.730	1.528	1.551
Total reflections	13336	9534	22317	14042	8461	19367	18264
Unique reflections	3128	4231	5315	6240	3740	4444	4314
R(int)	0.0275	0.0105	0.0166	0.0260	0.0477	0.0512	0.0370
Scan range θ [°]	2.51 to 28.32	1.92 to 28.24	1.75 to 28.32	1.82 to 28.29	2.75 to 28.30	1.94 to 28.28	2.09 to 28.29
Completeness to $\theta_{max.}$ [%]	93.0	94.9	93.4	95.3	98.5	94.8	93.9
Index ranges	$-11 \le h \le 11$	$-12 \le h \le 12$	$-30 \le h \le 30$	$-11 \le h \le 11$	$-9 \le h \le 10$	$-10 \le h \le 10$	$-11 \le h \le 11$
	$-19 \le k \le 19$	$-12 \le k \le 12$	$-18 \le k \le 18$	$-16 \le k \le 16$	$-18 \le k \le 18$	$-19 \le k \le 19$	$-14 \le k \le 15$
	$-13 \le l \le 13$	$-14 \le l \le 14$	$-19 \le l \le 19$	$-17 \le l \le 17$	$-10 \le l \le 10$	$-19 \le l \le 20$	$-22 \le l \le 22$
Data/restraints/parameters	3128/0/185	4231/0/260	5315/0/295	6240/0/325	3740/1/213	4444/0/258	4314/0/233
$R1$,[a][b] $wR2$ [$I > 4\sigma(I)$][c]	0.0477, 0.1314	0.0318, 0.0883	0.0298, 0.0827	0.0361, 0.0783	0.0930, 0.2637	0.0367, 0.0758	0.0333, 0.0826
$R1$,[a][d] $wR2$ (all data) [c] [d]	0.0540, 0.1377	0.0340, 0.0902	0.0323, 0.0852	0.0545, 0.0835	0.1191, 0.2836	0.0618, 0.0846	0.0412, 0.0875
Goodness-of-fit on F^2 [e]	1.039	1.051	1.076	1.042	1.083	1.018	1.079
Max./min. el. dens. [e.Å^{-3}]	0.360, −0.425	0.749, −0.429	0.354, −0.495	0.382, −0.484	3.918, −0.665	0.553, −0.456	0.496, −0.694

[a] $R1 = \Sigma||F_o| - |F_c||/\Sigma|F_o|$. [b] Denotes the value of the residual considering only the reflections with $I > 4\sigma(I)$. [c] $wR2 = \{\Sigma[w(F_o^2 - F_c^2)^2]/\Sigma[w(F_o^2)^2]\}^{1/2}$; $w = 1/[\sigma^2(F_o^2) + (aP)^2 + bP]$, $P = [\max(F_o^2 \text{ or } 0) + 2(F_c^2)]/3$. [d] Denotes the value of the residual considering all the reflections. [e] $S = [\Sigma w(F_o^2 - F_c^2)^2]/[(n - p)^{1/2}]$, n: number of data, p: parameters used.

complexes, particularly when stabilized by hydrogen bonding within solvated "cavities".[27] A similar observation of an *intramolecular* hydrogen bond between copper(II)-bound solvent molecules and pendant pyridyl moieties has been demonstrated by Mascharak et al. in the case of a ligand system incorporating an amide functionality.[28]

$[Cu(L1)_2(H_2O)_2](ClO_4)_2 \cdot 2DMF$ (1b)

The crystal structure of **1b** (Figure 3) displays similarities to that of **1a**. The geometry around the copper(II) coordination sphere in **1b** can also be described as elongated tetragonal [Cu(1)−(N2) = 2.0156(11) Å, Cu(1)−N(3) = 2.0175(11) Å, Cu(1)−O(1) = 2.3847(11) Å]. In this structure, there is a dihedral angle of 55.22° between the coordinated pyridyl rings of the two **L1** ligands. Furthermore, two water molecules occupy the axial sites of the copper(II) centre. They each form two strong hydrogen bonds; one *intramolecular* hydrogen bond to the pendant pyridyl "arm" [O(1)−N(4) = 2.8396(11) Å] and an *intermolecular* hydrogen bond to a DMF solvent molecule [O(1)−O(2)DMF = 2.7969(11) Å]. The copper(II) centre does not lie on an inversion centre and therefore the basal plane of the four equatorial nitrogen atoms does not form a perfect square basal plane.

In contrast to the well-known ligand tmpa (Scheme 1), there have been surprisingly few structurally characterised copper(II) complexes of tris(2-pyridyl)amine (tpa) reported in the literature; a search of the Cambridge Structural Data Base[29] reveals there to be only four.[30−33] In three of these four examples, two tpa ligands are found to be ligated to the copper(II) centre, while the other example is a larger tetrameric array.[33] In all the characterised structures, only two of the three pyridine nitrogen atoms are found to coordinate to the copper(II) centre. The single-crystal X-ray structures of the cations of **1a** and **1b** display similar features to those reported for the copper(II) complex $[Cu(tpa)_2(MeCN)_2](SO_3CF_3)_2$.[32] In this structure, the copper(II) ion is also found to occupy a crystallographic inversion centre. The tpa moiety coordinates to the copper(II) centre in an identical manner as observed for **L1**, and the two axial sites are occupied by acetonitrile solvent molecules. The third pyridine moiety of tpa remains uncoordinated. However, the crystal structures of **1a** and **1b** show one notable and interesting difference from that of $[Cu(tpa)_2(MeCN)_2](SO_3CF_3)_2$. The coordination of methanol molecules to the copper(II) centre of **1a** and of water molecules to the copper(II) centre in **1b** is stabilised by *intramolecular* hydrogen bonds formed between the coordinated solvent

Table 2. Selected bond lengths (Å) and angles (deg.) for compounds **1a−1d**, **2a**, and **2b**

1a					
Cu(1)−N(2)	2.0181(13)	Cu(1)−N(3)^{i}	2.0150(13)	Cu(1)−O(1)	2.4187(13)
Cu(1)−N(2)^{i}	2.0182(13)	Cu(1)−N(3)	2.0150(13)	Cu(1)−O(1)^{i}	2.4187(13)
N(3)−Cu(1)−N(3)^{i}	180.0	O(1)−Cu(1)−O(1)^{i}	180.0	N(3)−Cu(1)−N(2)	85.45(5)
N(2)−Cu(1)−O(1)^{i}	89.29(5)	N(2)−Cu(1)−O(1)	90.71(5)	N(3)−Cu(1)−N(2)^{i}	94.55(5)
N(3)−Cu(1)−O(1)	94.41(5)	N(3)−Cu(1)−O(1)^{i}	85.59(5)	N(2)^{i}−Cu(1)−O(1)^{i}	90.71(5)
Symmetry transformations used to generate equivalent atoms: −*x*, *y*, −*z*					
1b					
Cu(1)−N(2)	2.0156(11)	Cu(1)−N(3)^{i}	2.0174(11)	Cu(1)−O(1)^{i}	2.3847(11)
Cu(1)−N(2)^{i}	2.0156(11)	Cu(1)−N(3)	2.0175(11)	Cu(1)−O(1)	2.3847(11)
N(2)^{i}−Cu(1)−N(2)	92.10(6)	N(3)^{i}−Cu(1)−N(3)	96.86(6)	O(1)^{i}−Cu(1)−O(1)	176.12(6)
N(2)−Cu(1)−N(3)^{i}	175.56(4)	N(2)−Cu(1)−N(3)	85.64(5)	N(2)−Cu(1)−O(1)^{i}	86.06(4)
N(3)−Cu(1)−O(1)^{i}	87.03(4)	N(2)−Cu(1)−O(1)	96.64(4)	N(3)^{i}−Cu(1)−O(1)	87.03(4)
N(3)−Cu(1)−O(1)	90.40(4)				
Symmetry transformations used to generate equivalent atoms: −*x*, *y*, −*z* + 1/2					
1c					
Cu(1)−N(1)	2.0307(19)	Cu(1)−Cl(1)	2.2769(8)	Cu(1)−N(2)	2.0161(19)
Cu(1)−Cl(2)	2.2687(9)	Cu(1)−O(1)	2.2870(18)	Cu(2)−N(4)^{i}	1.988(2)
Cu(2)−N(4)	1.988(2)	Cu(2)−Cl(3)	2.2396(9)		
N(2)−Cu(1)−N(1)	84.31(8)	N(2)−Cu(1)−Cl(2)	90.05(6)	N(1)−Cu(1)−Cl(2)	168.79(5)
N(2)−Cu(1)−Cl(1)	170.07(6)	Cl(2)−Cu(1)−Cl(1)	93.20(3)	N(2)−Cu(1)−O(1)	93.57(8)
Cl(2)−Cu(1)−O(1)	100.93(6)	N(4)−Cu(2)−N(4)^{i}	180.0	N(4)−Cu(2)−Cl(3)	89.78(6)
N(4)−Cu(2)−Cl(3)^{i}	90.22(6)				
Symmetry transformations used to generate equivalent atoms: −*x*, −*y*, −*z*					
1d					
Cu(1)−N(1)	2.421(7)	Cu(1)−N(3)	2.027(5)	Cu(1)−N(3)^{i}	2.027(5)
Cu(1)−Cl(1)	2.2762(17)	Cu(1)−Cl(1)^{i}	2.2762(17)	N(3)−Cu(1)−N(3)^{i}	84.5(3)
N(3)−Cu(1)−N(1)	84.64(19)	N(3)−Cu(1)−Cl(1)^{i}	168.04(16)	N(3)−Cu(1)−Cl(1)	91.03(15)
Cl(1)^{i}−Cu(1)−Cl(1)	91.20(10)	Cl(1)−Cu(1)−N(1)	106.01(12)		
Symmetry transformations used to generate equivalent atoms: *x*, −*y* + 1/2, *z*					
2a					
Cu(1)−N(2)	1.982(2)	Cu(1)−N(3)	1.991(2)	Cu(1)−N(1)	2.073(2)
Cu(1)−Cl(1)	2.2265(7)	Cu(1)−O(1)	2.4837(7)	N(2)−Cu(1)−N(3)	161.15(9)
N(2)−Cu(1)−N(1)	83.89(8)	N(3)−Cu(1)−N(1)	81.39(8)	N(2)−Cu(1)−Cl(1)	98.87(7)
N(3)−Cu(1)−Cl(1)	99.47(6)	N(1)−Cu(1)−Cl(1)	154.73(6)	O(1)−Cu(1)−N(1)	104.39(6)
O(1)−Cu(1)−N(2)	82.88(7)	O(1)−Cu(1)−N(3)	89.43(7)	O(1)−Cu(1)−Cl(1)	100.87(7)
2b					
Cu(1)−N(2)	1.9798(17)	Cu(1)−N(3)	1.9836(17)	Cu(1)−Cl(1)	2.2619(6)
Cu(1)−Cl(2)	2.3271(6)	Cu(1)−N(1)	2.3399(17)		
N(2)−Cu(1)−N(3)	160.70(7)	N(2)−Cu(1)−Cl(1)	95.39(5)	N(3)−Cu(1)−Cl(1)	96.61(6)
N(2)−Cu(1)−Cl(2)	91.12(5)	N(3)−Cu(1)−Cl(2)	89.76(5)	Cl(1)−Cu(1)−Cl(2)	138.82(2)
N(2)−Cu(1)−N(1)	80.89(6)	N(3)−Cu(1)−N(1)	79.94(6)	Cl(1)−Cu(1)−N(1)	121.83(4)
Cl(2)−Cu(1)−N(1)	99.35(4)				

molecules and each pendant pyridyl "arm" as discussed above.

[$Cu_3(L1)_2(DMF)_2Cl_6$]·2DMF (1c)

Crystals of **1c** suitable for single-crystal X-ray diffraction analysis were grown over a period of a few days by slow diffusion of diethyl ether into a solution of the complex in DMF at room temperature. Single-crystal X-ray diffraction analysis revealed that **1c** crystallises in the triclinic space group $P\bar{1}$. The structure is shown in Figure 4, while the coordination parameters around the copper(II) centres are listed in Table 2.

The first striking observation is that the coordination complex contains more than one copper ion. The crystal structure reveals a ratio of three copper(II) ions to two **L1** molecules (Figure 4). The coordination geometry around

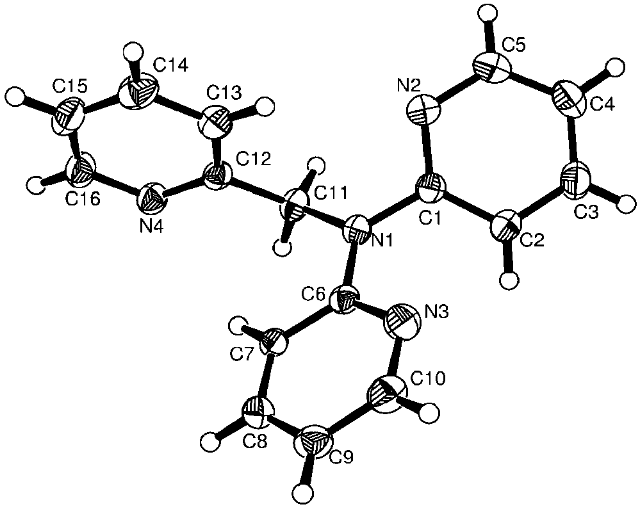

Figure 1. ORTEP representation (50% thermal probability ellipsoids) of the crystal structure of **L1**

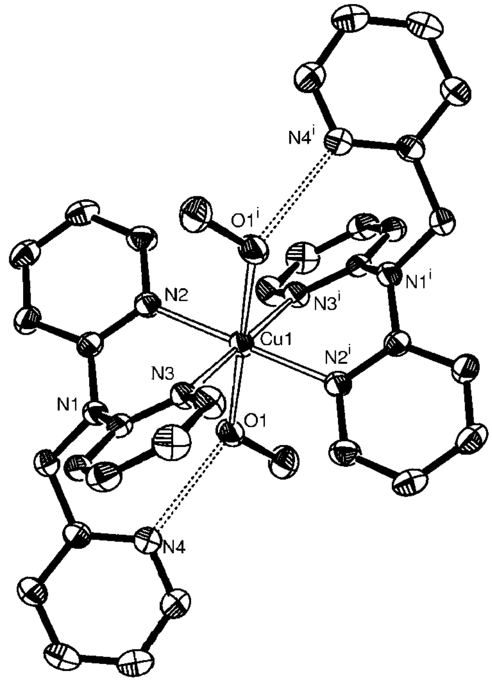

Figure 2. ORTEP representation (50% thermal probability ellipsoids) of the crystal structure of the cation of **1a**; perchlorate anions have been omitted for clarity

Cu(1) can be described as being close to square pyramidal, with N(1) and N(2) of the dipyridyl moiety of **L1** and two chloride anions, Cl(1) and Cl(2), forming the square basal plane [Cu(1)−N(2) = 2.0161(19) Å, Cu(1)−N(1) = 2.0307(19) Å, Cu(1)−Cl(2) = 2.2687(9) Å, Cu(1)−Cl(1) = 2.2769(8) Å]. The oxygen atom O(1) of a DMF solvent molecule occupies the axial position [Cu(1)−O(1) = 2.2870(18) Å]. The Cu(1) ion is found to be displaced from the basal plane by 0.179 Å. In common with the two previously described structures incorporating **L1**, N(4) of the third pyridyl arm is found not to coordinate to the Cu(1) centre. In contrast to the two previous structures, however, N(4) is unable to take part in *intramolecular* hydrogen bonding interactions with the coordinated anions and solvent molecule. Instead, N(4) coordinates to a second copper(II) ion in the structure, Cu(2) [Cu(2)−N(4) = 1.988(2) Å]. Cu(2) is found to occupy the crystallographic inversion centre of the unit cell. Another ligand of **L1** is coordinated through N(4)^{i} [related to N(4) by the operation of inversion at Cu(2)] to Cu(2). A chloride ion Cl(3) and its symmetry-equivalent Cl(3)^{i} complete the coordination sphere around Cu(2) [Cu(2)−Cl(3) = 2.2396(9) Å]. No other anions or DMF solvent molecules are found to occupy the vacant axial coordination sites of the Cu(2) centre. Due to the crystallographic restraint imposed on Cu(2), the coordination geometry around the Cu(2) ion can be rigor-

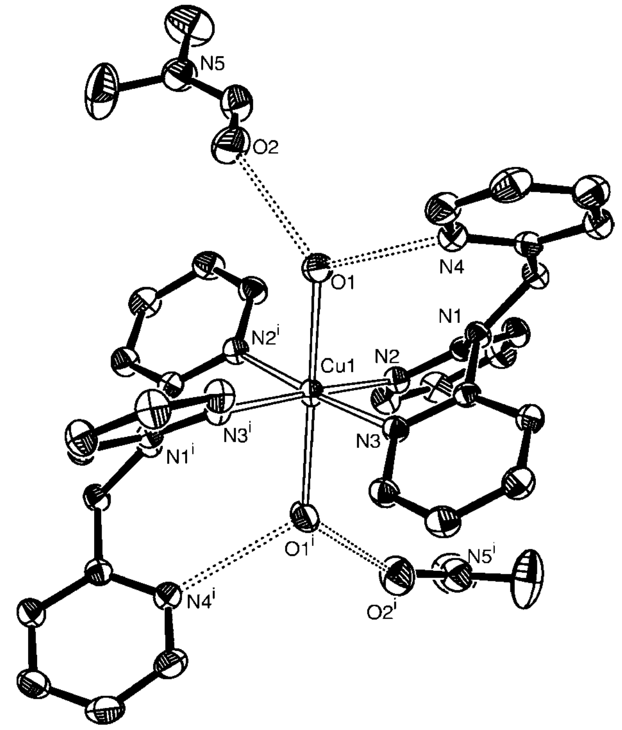

Figure 3. ORTEP representation (50% thermal probability ellipsoids) of the crystal structure of the cation of **1b**; perchlorate anions have been omitted for clarity

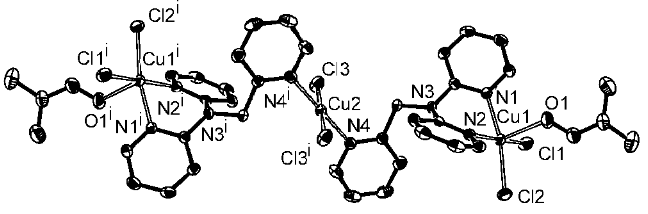

Figure 4. ORTEP representation (50% thermal probability ellipsoids) of the crystal structure of **1c**; two DMF solvent molecules have been omitted for clarity

ously defined as square planar. Two DMF solvent molecules (not shown) complete the structure.

$[Cu(L1)Cl_2]_n$ (1d)

Thin plate-like crystals of **1d** were grown by slow evaporation of the solvents from a solution of the complex in aqueous acetonitrile. The crystal structure is shown in Figure 5, while the coordination parameters around the copper(II) centre are listed in Table 2. During the refinement procedure, high residual electron densities were observed in the Fourier difference map. This is a direct result of the low crystal quality (possibly due to extremely thin plates being stuck together) resulting in high residual electron densities along the crystallographic twofold screw axis.

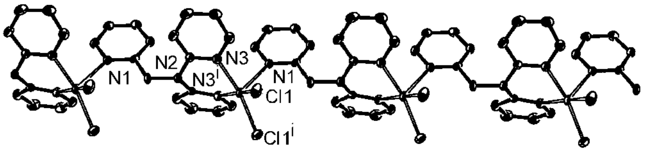

Figure 5. ORTEP representation (50% thermal probability ellipsoids) of the crystal structure of **1d**

The most striking feature is that **1d** has an infinite polymeric structure in the solid state. The ORTEP plot in Figure 5 shows three of the repeating units. The asymmetric unit cell consists of one half of a molecule of the formula "$[Cu(\mathbf{L1})Cl_2]$". The other symmetry-equivalent "half" of the structure is generated by reflecting the asymmetric unit contents through a mirror-plane consisting of the atoms Cu(1), N(1), N(2), and C(1)−C(6). The basal plane around each copper(II) centre in this structure is identical and is comprised of two pyridine nitrogen atoms of the dipyridyl moiety, N(1) and N(2), and two chloride anions, Cl(1) and Cl(2) [Cu(1)−N(1) = 2.033(14) Å, Cu(1)−N(2) = 2.014(14) Å, Cu(1)−Cl(2) = 2.275(5) Å, Cu(1)−Cl(1) = 2.276(5) Å]. The third pyridyl "arm" of **L1**, containing N(4), is not found to coordinate to the same copper(II) centre, as was seen in the structure of **1c**, but rather to a neighbouring copper(II) centre occupying the vacant axial position [N(4)−Cu(2) = 2.427(6) Å] and thus completing the distorted square-pyramidal coordination geometry around the copper(II) centre. No solvent molecules were found within the crystal lattice.

The two copper(II) chloride complexes of **L1** included in our study, **1c** and **1d**, show the effect of solvent coordination upon the nature of the final copper(II) complex obtained. Crystals of **1c**, the structure presented in Figure 4, were grown from a DMF-containing solution. In the crystal structure, DMF was found to occupy the axial site of the distorted square-pyramidal coordination environment of Cu(1) and consequently of its symmetry-equivalent Cu(1)^i as well.

On moving to a medium containing predominantly acetonitrile, crystals of **1d** were obtained, the structure of which is shown in Figure 5. Here, the crystal structure revealed that no solvent molecules are coordinated to the copper(II) centres. The structure of **1d** shows similarities to that of **1c** in that N(4) of the pendant pyridyl "arm" coordinates to a neighbouring copper(II) centre. However, in contrast to the structure of **1c**, the N(4) atom in **1d** is found to occupy the axial coordination position around the square-pyramidal copper(II) centres, previously occupied by a DMF molecule in **1c**. It is interesting to note that no bridging by the chloride ion takes place, a common occurrence in copper halide polymeric structures.

$[Cu(L2)(Cl)(ClO_4)]$ (2a)

Blue block-shaped crystals of **2a** suitable for single-crystal X-ray analysis were grown by slow diffusion of diethyl ether into a solution in acetonitrile. An ORTEP plot of the crystal structure is presented in Figure 6. Selected crystallographic data and bond angles and distances are listed in Table 1 and 2, respectively.

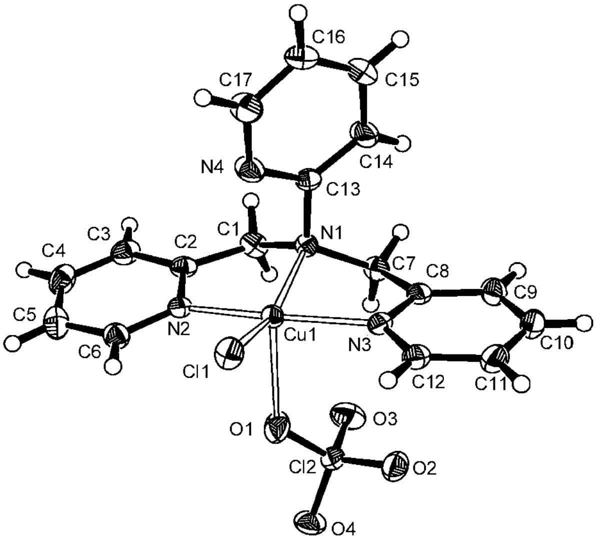

Figure 6. ORTEP representation (50% thermal probability ellipsoids) of the crystal structure of **2a**

As shown in Figure 6, two of the pyridyl rings of **L2** coordinate to the copper(II) centre in **2a**. The copper(II) centre is pentacoordinate, being coordinated by the pyridyl nitrogen atoms N(2) and N(3), the tertiary amine nitrogen N(1), chloride ion Cl(1), and O(1) of the perchlorate anion. The coordination environment around the copper(II) centre is best described as distorted square-pyramidal, with N(1), N(2), N(3), and Cl(1) forming the basal plane [Cu(1)−N(2) = 1.982(2) Å, Cu(1)−N(3) = 1.991(2) Å, Cu(1)−N(1) = 2.073(2) Å, Cu(1)−Cl(1) = 2.2265(7) Å] and O(1) of the perchlorate anion occupying the axial position [Cu(1)−O(1) = 2.4837(7) Å]. The coordination of the perchlorate anion in **2a** is also evident from the IR spectrum recorded from a Nujol mull. The strong band at

1089 cm^{-1} can be assigned as the coordinated perchlorate anion.

$[Cu(L2)Cl_2]\cdot H_2O$ (2b)

Green crystals suitable for single-crystal X-ray analysis were grown by slow evaporation of the solvents from a solution in aqueous methanol. An ORTEP plot of the crystal structure is displayed in Figure 7. Selected crystallographic data and bond lengths and angles are listed in Table 1 and 2, respectively.

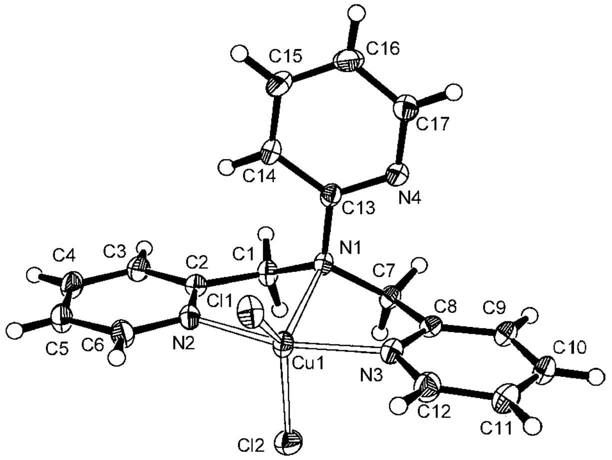

Figure 7. ORTEP representation (50% thermal probability ellipsoids) of the crystal structure of **2b**; a solvating water molecule has been omitted for clarity

As shown in Figure 7, and as was observed for **2a**, only two of the pyridyl rings of **L2** coordinate to the copper(II) centre in **2b**. The copper(II) centre is five-coordinate, being ligated by the pyridyl nitrogen atoms N(2) and N(3), the tertiary amine nitrogen N(1), and two chloride ions [Cu(1)−N(2) = 1.9798(17) Å, Cu(1)−N(3) = 1.9836(17) Å, Cu(1)−Cl(1) = 2.2619(6) Å, Cu(1)−Cl(2) = 2.3271(6) Å, Cu(1)−N(1) = 2.3399(17) Å]. At first sight, the geometry around the copper(II) centre might appear to be distorted trigonal bipyramidal, with the pyridyl nitrogen atoms N(2) and N(3) occupying the axial positions and the two chloride ions and N(1) occupying the equatorial plane. However, closer inspection reveals that the coordination environment around the Cu(1) centre is nearer to that found in square-pyramidal coordination complexes, with N(2), N(3), Cl(1), and Cl(2) forming the basal plane and the apical position being occupied by N(1). This is substantiated by examining the bond angles around the Cu(1) centre involving the atoms Cl(1), Cl(2), and N(1) [122°, 99°, 139° (sum = 360°)], which deviate from the value of 120° expected for a regular trigonal-bipyramidal geometry. Furthermore, the bond angle N(2)−Cu(1)−N(3) = 160.70(7)° is clearly less than 180°. This bond angle is a result of the small bite angles in each of the two five-membered chelate rings involving Cu(1), N(1), N(2), or N(3). These distortions and the value of the trigonality index τ of 0.36 (the index τ is zero for a square pyramid and unity for a trigonal bipyramid)[34] suggest that the coordination environment around Cu(1) is best described as trigonal-bipyramidal distorted square-based pyramidal (TBDSBP).

Ligand **L2** is a derivative of the parent amine (dipica) [dipica = bis(2-pyridylmethyl)amine] and shows a similar mode of coordination to copper(II) ions.[35−37] **L2** differs in that it possesses an additional pyridyl ring on the secondary aliphatic amine nitrogen atom, increasing the potential for additional coordination. There are numerous examples of derivatives of dipica, and the resulting ligands and metal complexes show interesting and novel properties.[38,39]

The structure of **2b** is similar to that reported for a copper complex of a derivatised dipica ligand.[38] This ligand was prepared by converting the secondary amine functional group of the precursor amine dipica into a tertiary amide group. The coordination parameters around the copper(II) centre are close to those seen in **2b**. In the structure, the tertiary amido nitrogen atom occupies the apical position at the copper(II) centre, with the other four ligating atoms (two pyridyl nitrogen atoms and two chloride ions) forming a distorted square plane in a similar manner to that shown in Figure 7. The coordination environment around the copper(II) centre is best described as trigonal-bipyramidal distorted square-based pyramidal (TBDSBP), having a trigonality index τ of 0.30.

UV/Vis Spectroscopy

The copper(II) complexes of **L2** are characterised by a rather broad d−d absorption band (ca. 650−1000 nm) in their solution (acetonitrile) electronic spectra; a low- or high-energy shoulder is often present as well, or occasionally two distinct absorption maxima are observed. In many cases, it has been demonstrated that the presence of a single d−d band with a low-energy shoulder is typical of a trigonal-bipyramidal geometry at copper, whereas an absorption with a high-energy shoulder indicates a square-pyramidal geometry. Examination of the electronic spectroscopic data of the copper(II) complexes of **L2** (see Exp. Sect.) indicates that, on the basis of this criterion, **2a** adopts a square-pyramidal geometry, whereas **2b** can best be described as having a geometry around the copper(II) centre close to trigonal bipyramidal. Complexes of **L1** are characterised by a rather broad absorption band at around 650 nm, indicating a square-pyramidal geometry in solution.

Electrochemistry

The half-wave potentials of complexes **1a**, **1d**, **2a**, and **2b** were determined by cyclic voltammetry in acetonitrile; the results are summarised in Table 3. All compounds displayed a reversible cyclic voltammogram, demonstrating that stable copper(I) complexes of the two ligands can be formed. Figure 8 shows the cyclic voltammogram of **2b**. Complexes with **L1** as a ligand are more easily reduced than those with **L2** as a ligand.

Table 3. Cyclic voltammetry of **1a**, **1d**, **2a**, and **2b** in acetonitrile

Compound[a]	E_p^{red} (V)	E_p^{ox} (V)	$E_{1/2}$ (V)	ΔE (mV)
1a	+0.31	+0.57	+0.44	260
1d	+0.31	+0.58	+0.45	270
2a	+0.11	+0.24	+0.18	130
2b	+0.07	+0.23	+0.15	160

[a] All potentials measured with a glassy carbon electrode vs. Ag/AgCl using $[NBu_4]PF_6$ (0.1 M) as electrolyte; scan rate: 100 mV s^{-1} in MeCN [$E_{1/2} = (E_p^{red} + E_p^{ox})/2$; $\Delta E = E_p^{ox} - E_p^{red}$].

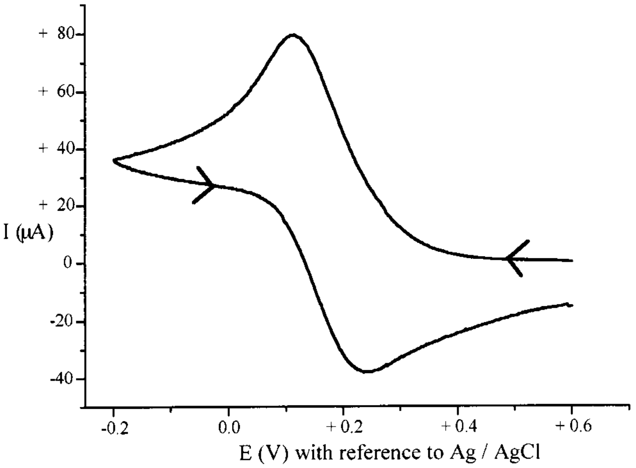

Figure 8. Cyclic voltammogram of **2b** in acetonitrile at 298 K; scan rate = 100 mV s^{-1}; concentration of complex = 1 mM; concentration of the supporting electrolyte $[NBu_4]PF_6$ = 0.1 M

Reactions of Dioxygen with Copper(I) Complexes of L1 and L2

As yet, we have been unable to isolate solid copper(I) complexes of **L1** or **L2**; only yellow-orange oils have been obtained. Therefore, to gain information on the reactions of dioxygen with the copper(I) complexes of **L1** or **L2**, these compounds were prepared in situ by mixing stoichiometric amounts of copper(I) salts with the ligands in acetone or propionitrile. Reactions of these solutions with dioxygen were investigated under the same conditions as employed for $[Cu(tmpa)(CH_3CN)]^+$ and its derivatives, using low-temperature stopped-flow techniques.[23] We observed that the copper complexes of both ligands were slowly oxidised, but in contrast to $[Cu(tmpa)(CH_3CN)]^+$ no "dioxygen adducts" were observed as intermediates.

Our earlier findings clearly demonstrated the influence of chelate ring size on the stability (or inertness) of copper "dioxygen" complexes.[23] $[Cu(tmpa)(CH_3CN)]^+$ reacts very rapidly with dioxygen to first form a superoxo complex, which reacts further to form a peroxo complex that is stable at low temperatures. Only one chelate ring is enlarged in $[Cu(pmea)]^+$, but we found that no superoxo complex could be detected in the course of its reaction with dioxygen; the initially formed peroxo complex rapidly underwent further reactions. In contrast to the findings for $[Cu(pmea)]^+$, a stopped-flow kinetic investigation showed that neither a superoxo nor a peroxo intermediate was observable during the reaction of $[Cu(pmap)]^+$ with dioxygen. $[Cu(tepa)]^+$ was found not to react with dioxygen. It was thus concluded that increasing the chelate ring size suppresses the formation of stable dioxygen adduct complexes in this series.

Unfortunately, reducing the chelate ring size by using **L1** or **L2** as described herein did not lead to a more stable copper superoxo or peroxo complex because intramolecular coordination of one of the pyridine donors was suppressed. The reaction of the copper(I) complex of tpa with dioxygen has been investigated previously and a cubane-like cluster was obtained as a product.[33] The authors did not report any dioxygen adduct complex as an intermediate during the course of this reaction.

Conclusions

We have reported the synthesis and characterisation of two new ligands, **L1** and **L2**, together with a series of copper(II) complexes derived from these ligands. The crystal structures of the complexes of **L1** demonstrate that in each case one of the three pyridyl donors remains uncoordinated, as observed in the copper complexes of tpa. However, the crystal structures of **1a** and **1b** show an important difference to copper tpa complexes: the coordination of methanol molecules to the copper(II) centre of **1a** and of water molecules in **1b** is stabilised by *intramolecular* hydrogen bonding between the coordinated solvent molecules and each pendant pyridyl "arm". Furthermore, using chloride as an anion in the syntheses of the copper(II) complexes of **L1** demonstrated an interesting solvent effect. In DMF, the trinuclear complex **1c**, incorporating coordinated DMF molecules is obtained, thus preventing the formation of a polymeric material. In contrast, in acetonitrile, no solvent molecules are coordinated and a polymeric complex **1d** is formed instead.

Ligand **L2** can be regarded as a derivative of bis(2-pyridylmethyl)amine (dipica) and the two complexes **2a** and **2b** are related to the complexes with dipica as ligand. **L2** differs from dipica in that it possesses a third pyridyl ring (not coordinated in **2a** and **2b**), increasing the potential for additional coordination.

As yet, it has not been possible to obtain copper(I) complexes of ligands **L1** or **L2** in a solid form, but reactions of dioxygen with these compounds formed in situ from a copper(I) salt and the ligand have been investigated. In contrast to the reaction of dioxygen with the copper(I) complex of tmpa, no dioxygen adducts could be observed as intermediates. Instead, complexes of both ligands were slowly oxidized to the copper(II) complexes, in line with their rather positive redox potentials.

Experimental Section

General Remarks: Reagents and solvents used were of commercially available reagent quality. Acetonitrile, propionitrile, diethyl ether, and acetone were dried by standard methods. $[Cu(CH_3CN)_4]ClO_4$ and $[Cu(CH_3CN)_4]PF_6$ were synthesized according to literature procedures.[40] The purities of the ligands were assessed by TLC, elemental analysis, and ^1H and ^{13}C NMR. UV/Vis spectra were measured on a Hewlett−Packard 8452 A spectrophotometer using standard 1 cm quartz cuvettes. ^1H and ^{13}C NMR spectra were recorded on a Bruker DXP 300 AVANCE spectrometer. Infrared spectra were recorded from samples in either Nujol mulls or KBr pellets on an ATJ Mattson Infinity 60 AR FT-IR instrument. Cyclic voltammetry was performed using an EG&G Model 263 potentiostat at 25 °C at a scan rate of 100 mV s^{-1}. The solutions under investigation contained 1 mM copper complex and 0.1 M $[NBu_4]PF_6$ in acetonitrile that had been deoxygenated by bubbling nitrogen through it. A conventional H-type cell was used, with glassy carbon, Pt, and Ag/AgCl as working, counter, and reference electrodes, respectively.

Variable-Temperature Stopped-Flow Measurements: Solutions of the complexes for the collection of time-resolved UV/Vis spectra were prepared in a glovebox and transferred to the low-temperature stopped-flow instrument by means of syringes. Dioxygen-saturated solutions were prepared by bubbling dioxygen through propionitrile or acetone in syringes (solubility of dioxygen in propionitrile at 25 °C is 0.0088 M,[20] while in acetone it is 0.0102 M[41]). The reactions were studied under pseudo-first-order conditions ([complex] < $[O_2]$), and time-resolved UV/Vis spectra of the reactions of dioxygen with copper(I) complexes were recorded with a modified Hi-Tech SF-3 L low-temperature stopped-flow unit (Salisbury, U.K.) equipped with a J&M TIDAS 16−500 photodiode-array spectrophotometer (J&M, Aalen, Germany).

Syntheses of Ligands and Complexes

Caution! Perchlorate salts are potentially explosive and should be handled with great care.

***N*-[(2-Pyridyl)methyl]-2,2′-dipyridylamine (L1):** Powdered potassium hydroxide (5.2 g, 93 mmol) was added to DMSO (40 mL). 2,2′-Dipyridylamine (3.42 g, 20 mmol) was added to this mixture. The resulting deep-orange coloured solution was stirred at room temperature for 45 min. 2-Picolyl chloride hydrochloride (3.28 g, 20 mmol) was then added and the orange solution was stirred at room temperature for 1 h. It was then diluted with water (50 mL), which led to the immediate deposition of a fine yellow precipitate. This precipitate was collected by filtration, washed with water (3 × 30 mL), and the yellow solid was recrystallised from hexane (75 mL) containing the minimum volume of dichloromethane. On cooling to 0 °C, fine yellow crystals formed. These were collected by filtration, washed with a little cold hexane, and dried to yield **L1** as a pale-yellow solid (2.9 g, 55%, 11 mmol). $C_{16}H_{14}N_4$: calcd. C 73.26, H 5.38, N 21.36; found C 73.31, H 5.50, N 21.23. M.p. 106−108 °C. FDI-MS: *m*/*z* = 262 $[M^+]$. ^1H NMR ($CDCl_3$, 300 MHz): δ = 5.60 (s, 2 H, $-CH_2-$), 6.82−6.86 (m, 2 H, ArH), 7.05−7.09 (m, 1 H, ArH), 7.24−7.32 (m, 3 H, ArH), 7.48−7.55 (m, 3 H, ArH), 8.28−8.30 (m, 2 H, ArH), 8.52 (d, 1 H, ArH). ^{13}C NMR ($CDCl_3$, 75 MHz): δ = 53.6, 114.4, 117.3, 121.2, 121.6, 136.5, 137.3, 148.2, 149.0, 156.8, 159.5. IR (KBr): ṽ = 3059 (w), 3004 (w), 2961 (w), 2925 (w), 2362 (w), 2337 (w), 1967 (w), 1943 (w), 1915 (w), 1893 (w), 1874 (w), 1845 (w), 1829 (w), 1796 (w), 1778 (w), 1737 (w), 1717 (w), 1701 (w), 1651 (w), 1585 (s), 1564 (m), 1470 (s), 1427 (s), 1379 (m), 1349 (m), 1325 (m), 1281 (m), 1260 (m), 1245 (m), 1225 (m), 1209 (m), 1173 (w), 1149 (m), 1130 (w), 1088 (m), 1044 (w), 983 (w), 901 (w), 873 (w), 772 (m), 753 (m), 737 (m), 661 (w), 612 (w), 585 cm^{-1} (w).

***N,N*-(2-Pyridyl)(2-pyridylmethyl)amine:** A solution of 2-pyridinecarboxaldehyde (9.2 mL, 96 mmol) and 2-aminopyridine (7.5 g, 80 mmol) in benzene (150 mL) was refluxed for 18 h with the continuous removal of water by means of a Dean−Stark trap. The solvent was subsequently removed in vacuo and the residue was taken up in absolute ethanol (200 mL). To this yellow solution, $NaBH_4$ (4.0 g, 105.8 mmol) was added and the solution was stirred at room temperature for 18 h. The excess $NaBH_4$ was then cautiously quenched by adding first water (100 mL) and then saturated aqueous NH_4Cl solution (100 mL) at 70 °C. Thereafter, the volatiles were removed in vacuo and the residue was redissolved in water (200 mL). The resulting aqueous solution was extracted with ethyl acetate (3 × 150 mL) and the combined organic fractions were dried over anhydrous magnesium sulfate. Upon removal of the solvent, a viscous yellow oil was obtained. The product was purified by vacuum distillation to yield a pale-yellow viscous liquid (6.0 g, 41%, 32.4 mmol). FDI-MS: *m*/*z* = 185 $[M^+]$. ^1H NMR ($CDCl_3$, 300 MHz): δ = 4.65 (d, 2 H, $-CH_2-$, $^3J_{H,H}$ = 5.3 Hz), 5.86 (br, 1 H, NH), 6.43−6.45 (m, 1 H, ArH), 6.53−6.58 (m, 1 H, ArH), 7.13−7.17 (m, 1 H, ArH), 7.30−7.40 (m, 2 H, ArH), 7.58−7.63 (m, 1 H, ArH), 8.09−8.11 (m, 1 H, ArH), 8.54−8.55 (m, 1 H, ArH). ^{13}C NMR ($CDCl_3$, 75 MHz): δ = 47.2, 107.7, 112.9, 121.6, 122.0, 136.6, 137.3, 147.9, 149.0, 158.3, 158.5. IR (KBr): ṽ = 3278 (br, m), 3084 (m), 3056 (m), 3018 (m), 2927 (w), 2865 (w), 1603 (s), 1571 (s), 1506 (s), 1490 (s), 1438 (m), 1332 (m), 1293 (m), 1254 (w), 1151 (m), 1120 (w), 1084 (w), 1049 (w), 983 (m), 771 (m), 686 (m), 611 (m), 527 cm^{-1} (m).

***N*-[Bis(2-pyridyl)methyl]-2-pyridylamine (L2):** Sodium hydride (60% dispersion in mineral oil; 1.3 g, 32.5 mmol) was added to anhydrous DMF (100 mL) under nitrogen. The resulting grey slurry was stirred at room temperature until hydrogen evolution had ceased (ca. 0.5 h). A solution of *N,N*-(2-pyridyl)(2-pyridylmethyl)amine (5.0 g, 27 mmol) in anhydrous DMF (60 mL) was then added dropwise to the sodium hydride slurry. The resulting orange solution was stirred until hydrogen evolution had ceased (ca. 1 h). To the amine carbanion, a solution of 2-picolyl chloride (free base) (3.79 g, 30 mmol) in anhydrous DMF (50 mL) was added dropwise and the brown solution was stirred overnight at room temperature. The light-orange solution obtained was then cautiously quenched by the addition of water (200 mL), and brine (50 mL) was also added. The aqueous solution was exhaustively extracted with dichloromethane (4 × 150 mL). The combined organic phases were washed with brine (200 mL) and dried over anhydrous magnesium sulfate. Removal of the solvent in vacuo yielded the crude product as a light-tan coloured solid. It was taken up in warm diethyl ether (100 mL), which led to the separation of a brown oil. The ethereal solution was decanted and the solvent was removed in vacuo. The crude cream-coloured product was recrystallised once from diethyl ether. On cooling to 0 °C, a fine white precipitate appeared, which was collected by filtration and dried in vacuo (5.3 g, 70%, 19.2 mmol). $C_{17}H_{16}N_4$: calcd. C 73.89, H 5.84, N 20.27; found C 73.94, H 5.97, N 20.03. M.p. 92−94 °C. FDI-MS: *m*/*z* = 276 $[M^+]$. ^1H NMR ($CDCl_3$, 300 MHz): δ = 4.99 (s, 4 H, $-CH_2-$), 6.47−6.61 (m, 2 H, ArH), 7.11−7.15 (m, 2 H, ArH), 7.22−7.25 (m, 2 H, ArH), 7.34−7.40 (m, 1 H, ArH), 7.55−7.60 (m, 2 H, ArH), 8.18 (d, 1 H, ArH), 8.54 (d, 2 H, ArH). ^{13}C NMR ($CDCl_3$, 75 MHz): δ = 54.1, 106.1, 112.7, 121.1, 122.0, 136.6, 137.5, 148.0, 149.4, 158.1, 158.7. IR (KBr): ṽ = 3046 (w), 3006 (w), 2964 (w), 2924 (w), 2924 (w), 2362 (w), 2338 (w), 1965 (w), 1916 (w), 1867 (w), 1843 (w), 1831 (w), 1768 (w), 1736 (w), 1719 (w), 1701 (w), 1596 (m), 1564 (m), 1492 (m), 1434 (m), 1391 (w), 1351 (m), 1283 (w), 1241 (w), 1180 (w), 1152 (w), 1094 (w), 1069 (w), 1047 (w), 976 (w), 938 (w), 884 (w), 848 (w), 779 (w), 753 (m), 664 (w), 635 (w), 615 (w), 589 (w), 568 (w), 545 cm^{-1} (w).

[Cu(L1)$_2$(CH$_3$OH)$_2$](ClO$_4$)$_2$ (1a): To a solution of **L1** (0.1 g, 0.38 mmol) in methanol (3 mL) was added a solution of Cu(ClO$_4$)$_2$·6H$_2$O (0.071 g, 0.19 mmol) in methanol (3 mL). Diethyl ether (100 mL) was then added, which led to the deposition of a fine blue precipitate. The mixture was stirred for a few minutes and then filtered. Dark-blue block-shaped crystals suitable for X-ray analysis were grown by slow evaporation of the solvents from a solution in aqueous methanol.

[Cu(L1)$_2$(H$_2$O)$_2$](ClO$_4$)$_2$·2DMF (1b): To a solution of **L1** (0.1 g, 0.38 mmol) in methanol (3 mL) was added a solution of Cu(ClO$_4$)$_2$·6H$_2$O (0.071 g, 0.19 mmol) in methanol (3 mL). Diethyl ether (100 mL) was then added, which led to the deposition of a fine blue precipitate. The mixture was stirred for a few minutes and then filtered. The precipitate was collected by filtration to give the crude product as a light-blue solid (0.135 g, 86%). Dark-blue block-shaped crystals suitable for X-ray analysis were grown by vapour diffusion of diethyl ether into a solution in DMF. $C_{32}H_{32}N_8CuCl_2O_{10}$: calcd. C 46.70, H 3.92, N 13.61; found C 46.49, H 3.83, N 13.36. UV/Vis [CH$_3$CN; λ_{max}, nm (ε, M^{-1} cm^{-1})]: 210 (8970), 250 (8847), 294 (8048), 410 (109), 656 (79).

[Cu$_3$(L1)$_2$(DMF)$_2$Cl$_6$] (1c): Ligand **L1** (0.10 g, 0.38 mmol) in DMF and CuCl$_2$·2H$_2$O (0.065 g, 0.38 mmol) in DMF (2 mL) were combined. Diethyl ether was then slowly allowed to diffuse into the resulting solution of **1c**. After a few days, blue/green block-shaped crystals of **1c** were formed.

[Cu(L1)Cl$_2$]$_n$ (1d): To a solution of **L1** (0.1 g, 0.38 mmol) in acetonitrile (3 mL) was added a solution of CuCl$_2$·2H$_2$O (0.066 g, 0.38 mmol) in methanol (5 mL). The mixture was stirred for a few minutes and then filtered. Crystals suitable for X-ray analysis formed soon thereafter (0.65 g, 50%).

[Cu(L2)Cl]ClO$_4$ (2a): To a solution of **L2** (0.1 g, 0.36 mmol) in methanol (10 mL) was added a solution of Cu(ClO$_4$)$_2$·6H$_2$O (0.067 g, 0.18 mmol) and CuCl$_2$·2H$_2$O (0.036 g, 0.18 mmol) in methanol (5 mL). The mixture was stirred for a few minutes and then filtered. Diethyl ether (100 mL) was quickly added to the filtrate, which led to the deposition of a sky-blue precipitate. This precipitate was collected by filtration and dried in vacuo to yield a light-green solid (0.16 g, 90%, 0.33 mmol). Crystals suitable for X-ray analysis were grown by vapour diffusion of diethyl ether into a solution in DMF. $C_{17}H_{16}N_4CuCl_2O_4$: calcd. C 43.01, H 3.82, N 11.80; found C 43.04, H 3.43, N 11.64. UV/Vis [CH$_3$CN, (ε, M^{-1} cm^{-1})]: λ_{max} = 214 (14372), 260 (20809), 366 (417), 708 nm (125).

[Cu(L2)Cl$_2$] (2b): To a solution of **L2** (0.1 g, 0.36 mmol) in methanol (10 mL) was added a solution of CuCl$_2$·2H$_2$O (0.062 g, 0.36 mmol) in methanol (5 mL). The mixture was stirred for a few minutes and then filtered. Diethyl ether (100 mL) was quickly added to the filtrate, which led to the deposition of a green precipitate. This precipitate was collected by filtration and dried in vacuo to yield a light-green solid (0.13 g, 86%, 0.31 mmol). Crystals suitable for X-ray analysis were grown from methanol/water (2:1; 10 mL). $C_{17}H_{16}N_4CuCl_2$: calcd. C 49.71, H 4.42, N 13.64; found C 49.87, H 4.15, N 13.50. UV/Vis [CH$_3$CN (ε, M^{-1} cm^{-1})]: λ_{max} = 212 (12735), 228 (11593), 260 (12801), 800 nm (320).

X-ray Crystallographic Study: Crystal data and experimental conditions are listed in Table 1. Selected bond lengths and bond angles with standard deviations in parentheses are presented in Table 2. Intensity data were collected on a Siemens SMART 1000 CCD diffractometer using graphite-monochromated Mo-K_α radiation (λ = 0.71073 Å). Exposure times were 10 s per frame for **L1**, **1a**, **1b**, and **1c** and 20 s per frame for **1d**, **2a**, and **2b**, collected using the ω-scan technique ($\Delta\omega$ = 0.45° for **L1**, **1a**, **1b**, and **1c** and 0.4° for **1d**, **2a**, and **2b**). The collected reflections were corrected for Lorentz, polarization, and absorption effects. The structures were solved by direct methods and refined by full-matrix least-squares methods on F^2.[42−44]

Crystallographic data (excluding structure factors) for the structures reported in this paper have been deposited with the Cambridge Crystallographic Data Centre as supplementary publication nos. CCDC-167124−167130. Copies of the data can be obtained free of charge on application to the CCDC, 12 Union Road, Cambridge CB2 1EZ, U.K. [Fax: (internat.) +44 (0)1223 336033; E-mail: deposit@ccdc.cam.ac.uk].

Acknowledgments

The authors gratefully acknowledge financial support from the DFG (S. Schindler) and the DAAD (S. P. Foxon), and Prof. Rudi van Eldik (University of Erlangen-Nürnberg) for his support of this work.

---

[1] K. D. Karlin, A. D. Zuberbühler, in *Bioinorganic Catalysis*, 2nd Edition (Eds.: J. Reedijk, E. Bouwman), Marcel Dekker, New York, **1999**, pp. 469−534.

[2] S. Fox, K. D. Karlin, in *Active Oxygen in Biochemistry* (Eds.: J. S. Valentine, C. S. Foote, A. Greenberg, J. F. Liebman), Blackie Academic and Professional, Chapman & Hall, Glasgow, **1995**, pp. 188−231.

[3] W. Kaim, J. Rall, *Angew. Chem.* **1996**, *108*, 47−64; *Angew. Chem. Int. Ed. Engl.* **1996**, *35*, 43−60.

[4] N. Kitajima, *Adv. Inorg. Chem.* **1992**, *39*, 1−77.

[5] N. Kitajima, Y. Moro-oka, *Chem. Rev.* **1994**, *94*, 737−757.

[6] K. D. Karlin, Z. Tyeklár (Eds.), *Bioinorganic Chemistry of Copper*, Chapman & Hall, New York, **1993**.

[7] E. I. Solomon, U. M. Sundaram, T. E. Machonkin, *Chem. Rev.* **1996**, *96*, 2563−2605.

[8] K. A. Magnus, H. Ton-That, J. E. Carpenter, *Chem. Rev.* **1994**, *94*, 727−735.

[9] M. E. Cuff, K. I. Miller, K. E. van Holde, W. A. Hendrickson, *J. Mol. Biol.* **1998**, *278*, 855−870.

[10] H. Decker, R. Dillinger, F. Tuczek, *Angew. Chem. Int. Ed.* **2000**, *39*, 1591−1595.

[11] J. P. Klinman, *Chem. Rev.* **1996**, *96*, 2541−2561.

[12] E. Spodine, J. Manzur, *Coord. Chem. Rev.* **1992**, *119*, 171−198.

[13] H.-C. Liang, M. Dahan, K. D. Karlin, *Curr. Opin. Chem. Biol.* **1999**, *3(2)*, 168−175.

[14] K. D. Karlin, *Science* **1993**, *261*, 701−708.

[15] A. G. Blackman, W. B. Tolman, in *Structure & Bonding: Metal-Oxo and Metal-Peroxo Species in Catalytic Oxidations* (Ed.: B. Meunier), Springer, Berlin, **2000**, vol. 97, pp. 179−211.

[16] S. Schindler, *Eur. J. Inorg. Chem.* **2000**, 2311−2326.

[17] R. R. Jacobson, Z. Tyeklár, A. Farooq, K. D. Karlin, S. Liu, J. Zubieta, *J. Am. Chem. Soc.* **1988**, *110*, 3690−3692.

[18] Z. Tyeklár, R. R. Jakobson, N. Wei, N. N. Murthy, J. Zubieta, K. D. Karlin, *J. Am. Chem. Soc.* **1993**, *115*, 2677−2689.

[19] M. J. Baldwin, P. K. Ross, J. E. Pate, Z. Tyeklár, K. D. Karlin, E. I. Solomon, *J. Am. Chem. Soc.* **1991**, *113*, 8671−8679.

[20] K. D. Karlin, N. Wei, B. Jung, S. Kaderli, P. Niklaus, A. D. Zuberbühler, *J. Am. Chem. Soc.* **1993**, *115*, 9506−9514.

[21] K. D. Karlin, S. Kaderli, A. D. Zuberbühler, *Acc. Chem. Res.* **1997**, *30*, 139−147.

[22] K. D. Karlin, D.-H. Lee, S. Kaderli, A. D. Zuberbühler, *Chem. Commun.* **1997**, 475−476.

[23] M. Schatz, M. Becker, F. Thaler, F. Hampel, S. Schindler, R.

R. Jacobsen, Z. Tyeklár, N. N. Murthy, P. Ghosh, Q. Chen, J. Zubieta, K. D. Karlin, *Inorg. Chem.* **2001**, *40*, 2312−2322.
[24] J. P. Wibaut, G. L. La Bastide, *Recl. Trav. Chim. Pays-Bas* **1933**, *52*, 493−498.
[25] W. Yang, L. Chen, S. Wang, *Inorg. Chem.* **2001**, *40*, 507−515.
[26] W. Yang, H. Schmider, Q. Wu, Y. Zhang, S. Wang, *Inorg. Chem.* **2000**, *39*, 2397−2404.
[27] C. J. Boxwell, P. H. Walton, *Chem. Commun.* **1999**, 1647−1648.
[28] J. M. Rowland, M. M. Olmstead, P. K. Mascharak, *Inorg. Chem.* **2000**, *39*, 5326−5332.
[29] F. H. Allen, J. E. Davies, J. J. Galloy, O. Johnson, O. Kennard, C. F. Macrae, E. M. Mitchell, G. F. Mitchell, D. G. Watson, *J. Chem. Inf. Comput. Sci.* **1991**, *31*, 187−204.
[30] P. A. Anderson, F. R. Keene, J. M. Gulbis, E. R. T. Tiekink, *Z. Kristall.* **1993**, *206*, 275−278.
[31] D. Boys, C. Escobar, W. Zamudio, *Acta Crystallogr., Sect. C* **1992**, *48*, 1118−1120.
[32] P. L. Dedert, J. S. Thompson, J. A. Ibers, T. M. Marks, *Inorg. Chem.* **1982**, *21*, 969−977.
[33] P. L. Dedert, T. Sorrell, J. A. Ibers, T. M. Marks, *Inorg. Chem.* **1982**, *21*, 3506−3517.
[34] A. W. Addison, T. N. Rao, J. Reedijk, J. van Rijn, G. C. Verschoor, *J. Chem. Soc., Dalton Trans.* **1984**, 1349−1356.
[35] H. J. Hoorn, P. de Joode, W. L. Driessen, J. Reedijk, *Recl. Trav. Chim. Pays-Bas* **1996**, *115*, 191−197.
[36] M. Palaniandavar, R. J. Butcher, A. W. Addison, *Inorg. Chem.* **1996**, *35*, 467−471.
[37] M. Palaniandavar, S. Mahadevan, M. Köckerling, G. Henkel, *J. Chem. Soc., Dalton Trans.* **2000**, 1151−1154.
[38] C. Cox, D. Ferraris, N. N. Murthy, T. Lectka, *J. Am. Chem. Soc.* **1996**, *118*, 5332−5333.
[39] N. Niklas, O. Walter, R. Alsfasser, *Eur. J. Inorg. Chem.* **2000**, 1723−1731.
[40] G. J. Kubas, B. Monzyk, A. L. Crumbliss, *Inorg. Synth.* **1979**, *19*, 90−92.
[41] P. Lühring, A. Schumpe, *J. Chem. Eng. Data* **1989**, *34*, 250−252.
[42] *Siemens Area Detector Absorption Correction, Siemens.*
[43] G. M. Sheldrick, *SHELX-97*, Universität Göttingen, **1997**.
[44] L. Zsolnai, *XPMA, ZORTEP*, Universität Heidelberg, **1997**.

Received July 24, 2001
[I01276]